ARTICLE
Journal of Cellular Biochemistry 115:1458–1466 (2014)

Journal of Cellular Biochemistry

Inhibition of AMPK/Autophagy Potentiates Parthenolide-Induced Apoptosis in Human Breast Cancer Cells

Can Lu,[1,2] Wenwen Wang,[1] Yongsheng Jia,[2] Xiaodong Liu,[2] Zhongsheng Tong,[2]** and Binghui Li[1]*

[1]*Laboratory of Cancer Cell Biology, Key Laboratory of Breast Cancer Prevention and Therapy, Tianjin Medical University Cancer Institute and Hospital, Tianjin 300060, P.R. China*

[2]*Department of Breast Oncology, Key Laboratory of Breast Cancer Prevention and Therapy, Tianjin Medical University Cancer Institute and Hospital, Tianjin 300060, P.R. China*

ABSTRACT

Parthenolide is the main bioactive component in feverfew, a common used herbal medicine, and has been extensively studied in relation to its anti-cancer properties. However there have been very few in-depth studies of the activities of this compound at the molecular level. Here, we showed that parthenolide increased reactive oxygen species (ROS), induced cell death, activated AMPK and autophagy, and led to M phase cell cycle arrest in breast cancer cells. Removal of ROS inhibited all parthenolide-associated events, such as cell death, AMPK activation, autophagy induction, and cell cycle arrest. Blockade of autophagy relieved cell cycle arrest, whereas inhibition of AMPK activity significantly repressed the induction of both autophagy and cell cycle arrest. These observations clearly showed that parthenolide-driven ROS activated AMPK-autophagy pathway. Furthermore, inhibition of either AMPK or autophagy significantly potentiated parthenolide-induced apoptosis. Therefore, our results show that parthenolide activates both apoptosis pathway and AMPK-autophagy survival pathway through the generation of ROS, and that suppression of AMPK or autophagy can potentially enhance the anti-cancer effect of parthenolide on breast cancer cells. J. Cell. Biochem. 115: 1458–1466, 2014.

KEY WORDS: PARTHENOLIDE; ROS; AUTOPHAGY; AMPK; APOPTOSIS

Breast cancer is one of the most common types of cancers among women in both developing and developed areas [Siegel et al., 2011]. Although recent progress in therapy has increased the survival of women with breast cancer, the further treatment available for patients still remains a big challenge, and this has boosted the extensive search for new targets and drugs.

In recent years, the search for effective plant-derived anti-cancer agents or their synthetic analogs has continued to gain interest in drug development. Among others, the sesquiterpene lactone, parthenolide (PTL), isolated from feverfew (Tanacetum parthenium) has been extensively studied in relation to its anti-cancer activities. PTL was reported in vitro to inhibit proliferation and induce apoptosis in various human cancers, such as colorectal cancer, breast cancer, hepatoma, cholangiocarcinoma, and pancreatic cancer [Zhang et al., 2004; Kim et al., 2005; Liu et al., 2010]. PTL-induced apoptosis was associated with inhibition of transcription factor nuclear factor-kappa B (NF-κB), mitochondrial dysfunction and increase of reactive oxygen species (ROS) [Wen et al., 2002; Guzman et al., 2005; Yip-Schneider et al., 2005; Wang et al., 2006; Zunino et al., 2007].

Autophagy is a highly regulated process that can be involved in the turnover of long-lived proteins and organelles [Levine and

Can Lu and Wenwen Wang contributed equally to this work.

Grant sponsor: National Natural Science Foundation of China; Grant numbers: 81171898, 81372185, 81302080; Grant sponsor: Anticancer Key Technologies R&D Program of Tianjin; Grant number: 12ZCDZSY16200; Grant sponsor: WU JIE PING Medical Foundation; Grant number: 320.6700.1139.

* Correspondence to: Binghui Li,Laboratory of Cancer Cell Biology, Key Laboratory of Breast Cancer Prevention and Therapy, Tianjin Medical University Cancer Institute and Hospital, Tianjin 300060, P.R. China.
E-mail: binghuili@tmu.edu.cn

** Correspondence to: Zhongsheng Tong, Department of Breast Oncology, Key Laboratory of Breast Cancer Prevention and Therapy, Tianjin Medical University Cancer Institute and Hospital, Tianjin 300060, P. R. China.
E-mail: 18622221181@163.com

Manuscript Received: 16 October 2013; Manuscript Accepted: 10 March 2014

Accepted manuscript online in Wiley Online Library (wileyonlinelibrary.com): 12 March 2014

DOI 10.1002/jcb.24808 • © 2014 Wiley Periodicals, Inc.

Kroemer, 2008]. Part of the cytoplasm and intracellular organelles are sequestered within characteristic double- or multimembraned autophagic vacuoles (named autophagosomes) and are finally delivered to lysosomes for bulk degradation. These superfluous, damaged, or aged cells or organelles are eliminated under various cellular stress conditions, and thus autophagy can be considered to assist cells to cope with unfavorable environments [Maiuri et al., 2007; Levine and Kroemer, 2008; Rubinstein and Kimchi, 2012]. On the other hand, autophagy can lead to programmed cell death in order to prevent further damage to surrounding healthy cells, given that the stress persists [Maiuri et al., 2007]. Therefore, autophagy can be involved in cell death or survival, depending on the environmental stimuli.

Autophagy can potentially cause resistance to therapeutic agents, a sort of chemical stress in essence [Aredia and Scovassi, 2013; Jain et al., 2013]. Here, we show that PTL induces autophagy through ROS-AMPK pathway, and that the inhibition autophagy or AMPK promotes PTL-induced apoptosis in MCF-7 breast cancer cells.

MATERIALS AND METHODS

CHEMICALS AND REAGENTS

Parthenolide (PTL), N-acetyl-L-cysteine (NAC), rotenone, compound C and 3-Methyladenine (3-MA) were obtained from Sigma (USA). NAC, an antioxidant, were dissolved in the growth medium. PTL, rotenone, compound C and 3-MA were dissolved in DMSO as a stock buffer. ROS dyes H2DCFDA (5-(and-6)-chloromethyl-2′7′-dichlorodihydrofluorescein diacetate acetyl ester) and DNA staining fluorescent dye Hoechst 33258 were obtained from Invitrogen (USA).

GENE CONSTRUCTION

The cDNA of EGFP-fused LC3, an autophagy probe, was generated by PCR, and the cDNA of mAG-hGem(1/110), a cell cycle probe, was commercially synthesized (Genewiz, China) as described previously [Sakaue-Sawano et al., 2008]. VC3AI, an apoptosis indicator, was described in detail in our previous report [Zhang et al., 2013]. All cDNAs were cloned into lentiviral expression vectors, pCDH-puro-CMV or pCDH-Neo-CMV using the eFusion Recombinant Cloning Kit (Biophay, China). The pLKO.1 lentiviral RNAi expression system was used to construct lentiviral shRNA for AMPKα. The sequences of shRNA used in this study included the following:

shScramble: CCGGCCTAAGGTTAAGTCGCCCTCGCTCGAGCGAGGGCGACTTAACCTTAGGTTTTT

shAMPKα1/2: CCGGATGATGTCAGATGGTGAATTTCTCGAGAAATTCACCATCTGACATCATTTTTT

CELL CULTURE

MCF-7 breast cancer cells were maintained in DMEM (high glucose) supplemented with 10% fetal bovine serum (Hyclone, USA) and 50 IU penicillin/streptomycin (Invitrogen), and MCF-10A cells were cultured in DMEM/F12 containing 5% horse serum (Hyclone), 20 ng/ml EGF (Roche, USA), 0.5 mg/ml hydrocortisone (Sigma, USA), 100 ng/ml cholera toxin (Sigma), 10 μg/ml insulin (Sigma) and 50 IU penicillin/streptomycin (Invitrogen) in a humidified atmosphere with 5% CO_2 at 37°C.

ROS ANALYSIS

Intracellular ROS production was monitored by the permeable fluorescence dye, H2DCFDA. H2DCFDA can readily react with ROS to form the fluorescent product 2,7-dichlo-rofluorescein (DCF) [Robinson et al., 1994]. The intracellular fluorescence intensity of DCF is proportional to the amount of ROS generated by the cells [Huang et al., 2002]. After the indicated treatment, the cells were incubated with 10 μM of H2DCFDA dissolved in PBS for 30 min and then cells were harvested and resuspended in PBS (10^6 cells/ml). The fluorescence intensity of intracellular DCF (excitation 488 nm, emission 530 nm) was measured using FACScan (BD Biosciences, USA).

IMAGING OF CULTURED CELLS

For live cell imaging, cells were grown in six-well plates, and after the desired treatments, the fluorescence and phase-contrast imaging was captured with a Nikon Eclipse TE2000-U fluorescence microscope (Nikon, Japan).

For fixed cell imaging, after the desired treatments, cells grown in six-well plate were fixed with 4% paraformaldehyde in PBS for 30 min, and then carefully washed twice with PBS buffer. The fixed cells were incubated with 2 μg/ml of Hoechst33258 for 5 min for nuclear DNA staining. After washing twice with PBS, the cells were imaged.

CELL DEATH ASSAY

After desired treatments, cells grown in plates were fixed, stained with Hoechst 33258 (Sigma) and imaged as described above. Cells containing condensed chromatins were counted as dead.

As for apoptosis, VC3AI probe was used. VC3AI can be activated by active caspase-3-like proteases and display fluorescence. Therefore, after MCF-7 cells stably expressing VC3AI were treated as indicated, the fluorescent cells were counted as apoptotic [Zhang et al., 2013].

CELL CYCLE ANALYSIS

For FACS analysis, after desired treatments, MCF-7 cells were trypsinized to single cells, and then washed twice with PBS. One milliliter of cells (about 10^6 cells) was aliquoted in a 15 ml polypropylene tube and 3 ml of cold absolute ethanol was added dropwise while vortexing. Cells were fixed overnight at 4°C, washed twice with PBS, and then incubated with 1 ml of PI staining buffer (10 mM Tris pH 7.5, 5 mM $MgCl_2$, 20 μg/ml RNAse A and 5 μg/ml PI) for 30 min at 37°C. Cells were analyzed using a FACScan (BD Biosciences, USA). Cell cycle distribution was analyzed using FlowJo (6.0) software (Tree Star).

For fluorescent probe analysis, mAG-hGem(1/110) was used to analyze M phase of MCF-7 cells. mAG-hGem(1/110) is a fluorescent protein mAG harnessed to antiphase oscillating protein that mark cell-cycle transitions, and thus it is a cell-cycle-dependent biosensor and indicates dividing cells by fluorescence. After MCF-7 cells stably expressing mAG-hGem(1/110) were treated as indicated, the fluorescent round cells were the cells arrested in M phase [Sakaue-Sawano et al., 2008].

WESTERN BLOT

After desired treatments as specified as indicated, cells were washed twice with PBS and lysed in buffer (20 mM Tris-HCl, pH 7.5, 150 mM

NaCl, 1 mM EDTA, 1% Triton X-100, 2.5 mM sodium pyrophosphate, 1 mM b-glycer-ophosphate, 1 mM sodium vanadate, 1 mg/ml leupeptin, 1 mM phenylmethyl-sulfonylfluoride). Equal amounts of protein (30 μg) were loaded onto 15% SDS–PAGE gels. Western detection was carried out using a Li-Cor Odyssey image reader (Li-Cor, USA). Anti-LC3, anti-AMPK, anti-p-AMPK, and anti-β-actin antibodies were obtained from Cell Signaling Technology (USA). All these primary antibodies were used with a dilution of 1:1,000. The goat anti-mouse immunoglobulin G (IgG) and goat anti-rabbit IgG secondary antibodies were obtained from Li-Cor. The final concentration of the secondary antibodies used was 0.1 μg/ml.

LENTIVIRUS PRODUCTION

Viral packaging was done according to a previously described protocol [al Yacoub et al., 2007]. Briefly, expression plasmids pCDH-CMV-cDNA, pCMV-dR8.91, and pCMV-VSV-G were co-transfected into 293T cells using the calcium phosphate coprecipitation at 20:10:10 μg (for a 10-cm dish). The transfection medium containing calcium phosphate and plasmid mixture was replaced with fresh complete medium after incubation for 5 h. Media containing virus was collected 48 h after transfection and then concentrated using Virus Concentrator Kit (Biophay, China). The virus was resuspended in the appropriate amount of complete growth medium and stored at −80°C. Cancer cells were infected with the viruses at the titer of 100% infection in the presence of polybrene (10 μg/ml) for 48 h, and then cells were selected with puromycin or neomycin.

RESULTS

PTL INDUCES CELL DEATH IN BREAST CANCER CELLS BY INCREASING ROS LEVEL

Consistent with previous reports that PTL displayed potent anti-cancer effects and induced cell death [Gunn et al., 2011; Mathema et al., 2012], treatment of PTL induced significant level of cell death in MCF-7 breast cancer cells but not in non-transformed mammary epithelial cells, MCF-10A (Fig. 1a), indicating its specific effect on cancer cells. Since PTL had been reported to induce ROS generation in some cancer cells [Guzman et al., 2005; Wang et al., 2006; Zunino et al., 2007], we further characterized the effect of PTL on the generation of ROS in MCF-7 cells using fluorescent dye, H2DCFDA. Indeed, treatment of MCF-7 cells with PTL led to ROS accumulation in a concentration-dependent manner (Fig. 1b). After 5 h of PTL treatment, an increase of two- to threefold in ROS was observed in MCF-7 cells (Fig. 1b). ROS is often linked with the induction of cell death, and therefore we investigated the effect of increased ROS level on cell death of PTL-treated MCF-7 cells using a common antioxidant, NAC. As shown in Figure 1a,b, NAC significantly

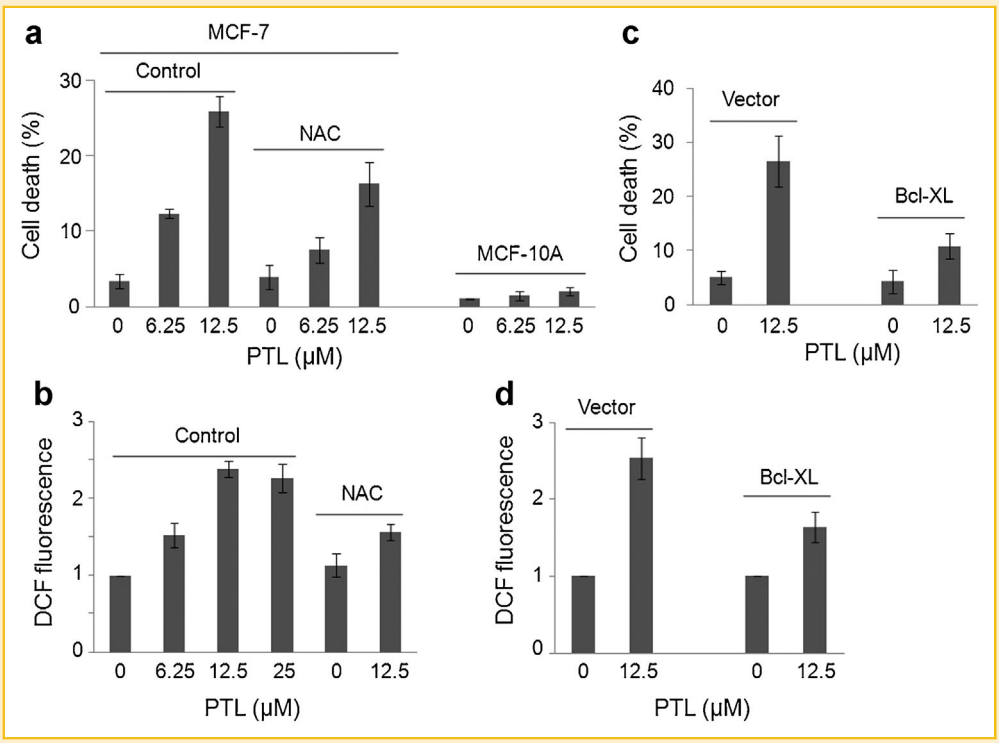

Fig. 1. PTL induced cell death and ROS generation in breast cancer cells. a: MCF-7 and MCF-10A cells were treated with different concentrations of PTL for 48 h in the presence or absence of 10 mM of NAC, an antioxidant, and then cell death was determined. b: MCF-7 breast cancer cells were treated with different concentrations of PTL for 5 h in the presence or absence of 10 mM of NAC, and then ROS was determined. c: MCF-7 cells stably expressing empty vector or human Bcl-XL were treated with PTL for 5 h, and then ROS was determined. d: MCF-7 cells stably expressing empty vector or human Bcl-XL were treated PTL for 48 h, and then cell death was determined. Error bar in all panels indicates ± SD (n = 3).

reduced ROS level and meantime suppressed cell death in MCF-7 cells treated with PTL. ROS can leak out of the mitochondria or be generated in the cytoplasm. To figure out the main source of ROS, we expressed Bcl-XL protein in MCF-7 cells. Bcl-XL protects the mitochondrial membrane potential, suppresses mitochondria-driven ROS and thus represses cell death. Our results showed that Bcl-XL expression obviously inhibited PTL-induced ROS and cell death in MCF-7 cells (Fig. 1c,d). These results strongly suggested that PTL-induced cell death in MCF-7 cells was mediated by the elevated level of ROS that mainly come from the mitochondria.

PTL INDUCES AUTOPHAGY IN BREAST CANCER CELLS

Because it had reported that PTL induced apoptosis in some cancer cells [Cheng and Xie, 2011; Kim et al., 2012; Wyrebska et al., 2013], we characterized the cell death of MCF-7 cells treated with PTL. We stably expressed an apoptosis biosensor, VC3AI, in MCF-7 cells. VC3AI, Venus-based caspase-3-like activity indicator, contains a capase-3 cleavage site and acquires fluorescent activity only after cleavage by activated caspase-3-like proteases, and thus it can veridically indicate caspase-3-like activity, a well-characterized event of apoptosis [Zhang et al., 2013]. As a positive control, we treated MCF-7/VC3AI cells with TNF-α for 48 h, and all the dead cells showed significant Venus fluorescence (Fig. 2a,b), consistent with our previous report [Zhang et al., 2013]. In contrast, some of dead MCF-7 cells treated with PTL for 48 h were non-fluorescent (Fig. 2a,b), suggesting the presence of non-apoptotic cell death.

Typically, cell death includes three types, apoptosis, necrosis, and autophagy [Edinger and Thompson, 2004]. Since we observed the shrunk morphological change in dead cells without fluorescence (Fig. 2a), in contrast to the swelled morphological shape in necrotic cells [Edinger and Thompson, 2004], we investigated the involvement of autophagy in PTL-induced cell death in MCF-7 cells. The microtubule-associated light chain 3 (LC3) is incorporated into autophagosome upon autophagy induction, which can be visualized by the foci formation of a GFP tagged LC3 (GFP-LC3) [Kimura et al., 2007]. When MCF-7 cells expressing GFP-LC3 were treated with PTL for 18 h, significant level of GFP-LC3 foci was observed (Fig. 2c). Since ROS was reported to activate autophagy in some conditions, we examined whether PTL-induced ROS contributed to this autophagic progress. As shown in Figure 2d, antioxidant NAC significantly blocked PTL-induced GFP-LC3 foci in MCF-7 cells (Fig. 2d).

To further confirm the involvement of autophagy in PTL-treated MCF-7 cells, we detected the level of LC3 protein. LC3 is cleaved

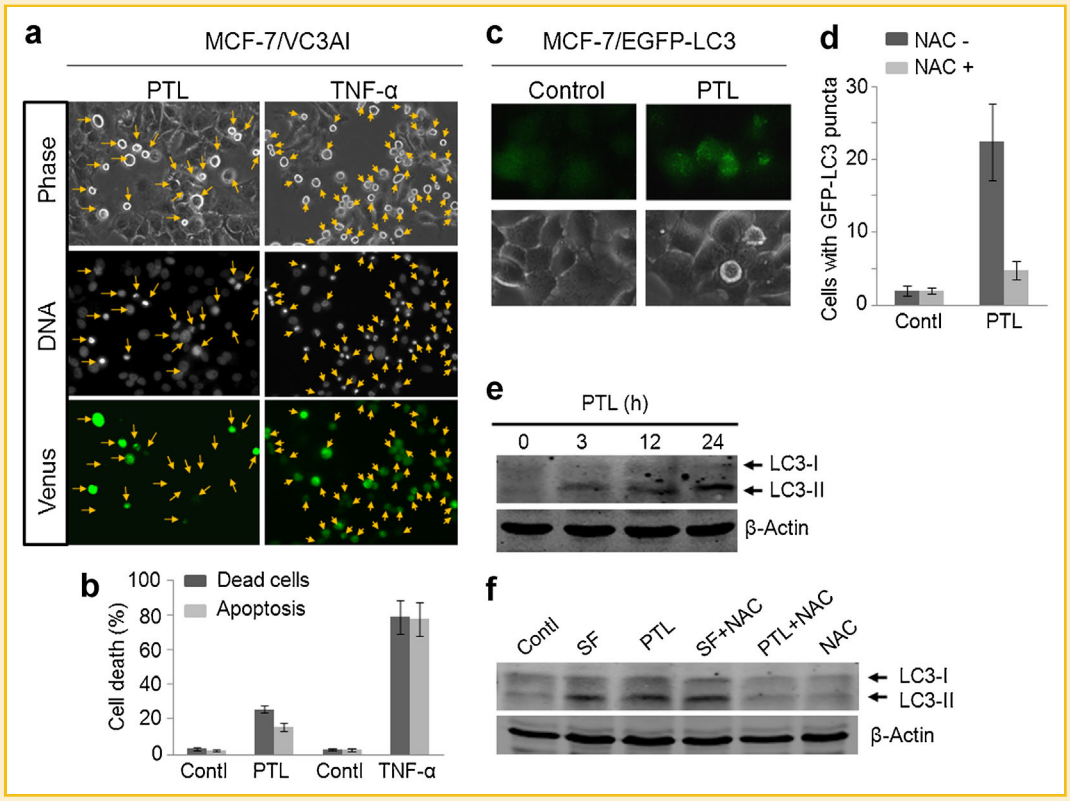

Fig. 2. PTL induced autophagy in breast cancer cells. a: MCF-7 cells expressing VC3AI were treated with 12.5 μM of PTL or 20 ng of TNF-α for 48 h, and then were fixed for DNA staining with Hoechst 33258. DNA staining indicates cell death (arrows) and Venus fluorescence from activated VC3AI indicates apoptosis. b: The fraction of dead or apoptotic MCF-7/VC3AI cells after treatment as described in (a). Error bar indicates ± SD (n = 3). c: MCF-7 cells expressing EGFP-LC3 were treated with 12.5 μM of PTL for 18 h and were imaged with a fluorescence microscope. d: The fraction of cells with GFP foci was determined after treatment as described in (c). Error bar indicates ± SD (n = 3). e: MCF-7 cells were treated with 12.5 μM of PTL for the indicated periods, and LC3-I/II protein levels were determined by Western blot analysis. f: MCF-7 cells were treated as indicated for 24 h, and LC3-I/II protein levels were determined by Western blot analysis. Serum-free (SF) treatment was used as a positive control for autophagy induction.

during autophagy to form the faster migrating LC3-II form. As shown in Figure 2e, significant levels of LC3-II were detected after 24 h of PTL treatment. At the same time, our results showed that NAC obviously repressed the PTL-activated LC3-II but did not affect LC3-II level induced by serum deprivation that elicited autophagy (Fig. 2f). Taken together, these data strongly demonstrated that PTL promoted ROS generation and then induced autophagy in MCF-7 cells.

INHIBITION OF AUTOPHAGY POTENTIATES PTL-INDUCED APOPTOSIS IN BREAST CANCER CELLS

Autophagy induced by persistent stress can finally lead to cell death, at least in part including apoptosis [Rubinstein and Kimchi, 2012]. Therefore, we investigated whether PTL-induced cell death in MCF-7 cells resulted from autophagy. 3-MA is a widely used cell-permeable autophagy inhibitor and it blocks autophagosome formation during the early stage [Seglen and Gordon, 1982]. Surprisingly, 3-MA completely shifted cell death to apoptosis (Fig. 3a), and meantime significantly increased cell death (apoptosis) (Fig. 3a, compared to data in Fig. 1a) in MCF-7 cells treated with PTL. As expected, 3-MA apparently suppressed PTL-induced autophagy (Fig. 3c). These data suggest that upon PTL treatment, MCF-7 cells try to conquer the surrounding chemical stress through autophagy to survive.

PTL INDUCES CELL CYCLE ARREST IN BREAST CANCER CELLS

During the course of investigation, we found that PTL induced round morphology in many MCF-7 cells even after 8 h of treatment, and these round cells did not undergo apoptosis as indicated by VC3AI (Fig. 4a). More importantly, most of these round cells restored their growth upon the deprivation of PTL at 8 h (data not shown). This suggests that these round cells just stayed in an adaptive state to avoid chemical stress, and will resuscitate upon the removal of nasties.

The disadvantageous conditions often lead to cell cycle arrest with round cellular morphology in G2/M phase, and thus we analyzed cell cycle in the PTL-treated MCF-7 cells. As analyzed by the flow cytometry (Fig. 4b), PTL reduced the fraction of cells in G1 phase while increased that in G2/M by about two folds, indicating that PTL led to the cell cycle arrest in G2/M phase. However, this result did not exactly reflect the morphological difference between the PTL-treated and control MCF-7 cells we observed. In fact, PTL induced much more round cells than the control (Fig. 3a). As the flow cytometry was not able to distinguish the cells in G2 and M phases, we decided to use a genetically encoded fluorescent probe, mAG-hGem(1/110) [Sakaue-Sawano et al., 2008]. mAG-hGem(1/110) is the fluorescent protein mAG harnessed to antiphase oscillating protein that marks cell-cycle transitions, and thus it is a cell-cycle-dependent biosensor and indicates dividing cells by fluorescence. The expression of mAG-hGem(1/110) can characterize cells in M phase with fluorescence and round morphology (Fig. 4c) [Sakaue-Sawano et al., 2008]. We treated MCF-7/mAG-hGem(1/110) cells with PTL for 8 h, and observed a sixfold increase in the number of fluorescent round cells arrested in M phase (Fig. 4d,e). Therefore, PTL mainly inhibited the mitosis of MCF-7 cells. Rotenone, an inhibitor of electron transport chain in mitochondria, can induce G2/M arrest [Armstrong et al., 2001]. Here, as a positive control, rotenone indeed enhanced the portion of cells in M phase (Fig. 4d,e). Although MCF-7 cells arrested in M phase did not virtually undergo cell death after 8 h of

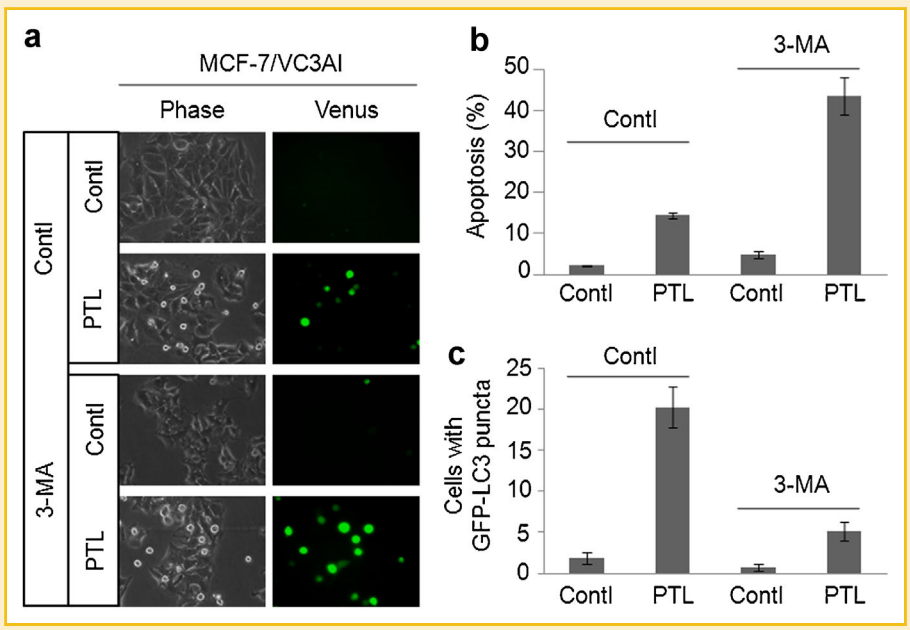

Fig. 3. Inhibition of autophagy potentiated PTL-induced apoptosis in breast cancer cells. a: MCF-7 cells expressing VC3AI were treated with 12.5 μM of PTL for 48 h in the presence or absence of 5 mM of 3-MA, an inhibitor of autophagy, and were imaged with a fluorescence microscope. b: The fraction of apoptotic cells after treatment as described in (a). Error bar indicates ± SD (n = 3). c: The fraction of cells with GFP foci was determined after MCF-7 cells expressing EGFP-LC3 were treated with 12.5 μM of PTL for 18 h in the presence or absence of 5 mM of 3-MA. Error bar indicates ± SD (n = 3).

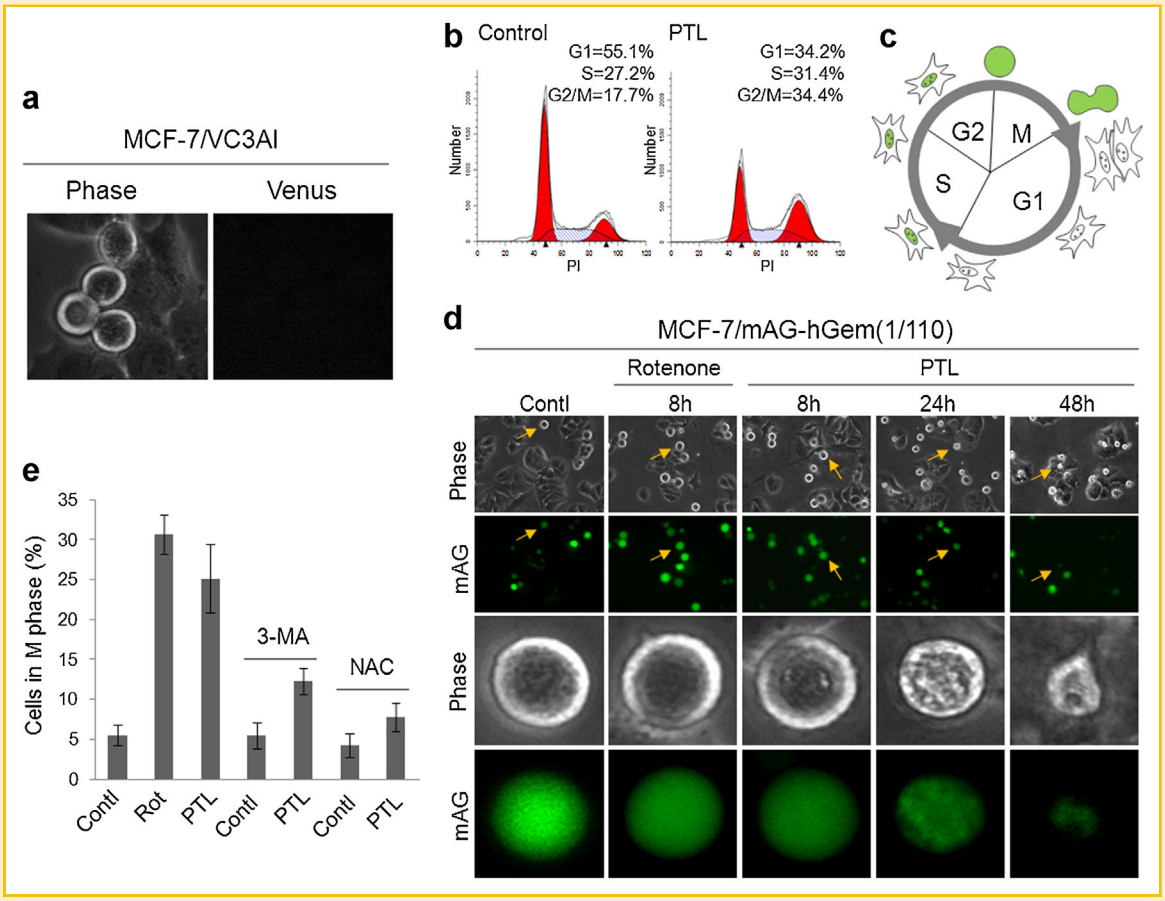

Fig. 4. PTL induced cell cycle arrest in breast cancer cells. a: MCF-7 cells expressing VC3AI were treated with 12.5 μM of PTL for 8 h, and were imaged with a fluorescence microscope. b: Cell cycle of MCF-7 cells treated with control or 12.5 μM of PTL for 8 h was analyzed by FACS. c: A fluorescent probe, mAG-hGem(1/110), that labels S/G2/M phase nuclei green, from Sakaue-Sawano et al. (2008). The single round green cells were those arrested in M phase. d: MCF-7 cells expressing mAG-hGem(1/110) were treated with 12.5 μM of PTL for different time, or with 1 μM of rotenone for 8 h, and were imaged with a fluorescence microscope. e: The fraction of MCF-7/mAG-hGem(1/110) cells after treatments as indicated. Error bar indicates ± SD (n = 3).

PTL treatment, they finally died given the persistent presence of treatment (Fig. 4d).

Furthermore, our data showed that both 3-MA and NAC significantly decreased PTL-induced cell cycle arrest (Fig. 4e). These data showed that PTL-promoted ROS and autophagy preceded cell cycle arrest in MCF-7 cells.

AMPK PATHWAY IS INVOLVED IN PTL-INDUCED AUTOPHAGY

The induction of ROS, autophagy and cell cycle arrest in MCF-7 cells by PTL strongly implicated the presence of metabolic stress. Therefore, we investigated the role of AMPK, a kinase involved in metabolic stress, in PTL-treated MCF-7 cells. AMPK could be activated via many pathways including ROS [Russo et al., 2013; She et al., 2014]. The time-course results showed that PTL obviously increased the level of phosphorylated AMPK protein in the very early stages (Fig. 5a). PTL induced an increase of 1.5- to 2-fold in AMPK phosphorylation during 6 h, and NAC significantly blocked PTL-promoted AMPK phosphorylation, suggesting the contribution to AMPK activation by PTL-driven ROS. In the meantime, we found that compound C, a selective inhibitor of AMPK, decreased the number of cells in M phase, suppressed autophagy, and synergically increased apoptosis in PTL-treated MCF-7 cells (Fig. 5b–d).

To further confirm the role of AMPK pathway in PTL-treated MCF-7 cells, we depleted AMPK expression level using a lentiviral knockdown construct, shAMPK (Fig. 5e). Consistent with the results obtained with compound C, the knockdown of AMPK attenuated PTL-induced cell cycle arrest and autophagy while exacerbated PTL-induced apoptosis (Fig. 5f–h). In addition, our data showed that AMPK knockdown inhibited the active turnover of LC3, and thus confirmed the requirement of AMPK for PTL-induced autophagy. Taken all together, our data strongly demonstrated that AMPK pathway was involved in PTL-induced cell cycle arrest, autophagy and cell death in MCF-7 breast cancer cells (Fig. 6).

DISCUSSION

The sesquiterpene lactone, PTL, is the main bioactive component in feverfew, an herbal medicine used for fever, migraine, and arthritis [Knight, 1995], and shows a strong anti-cancer activity against a

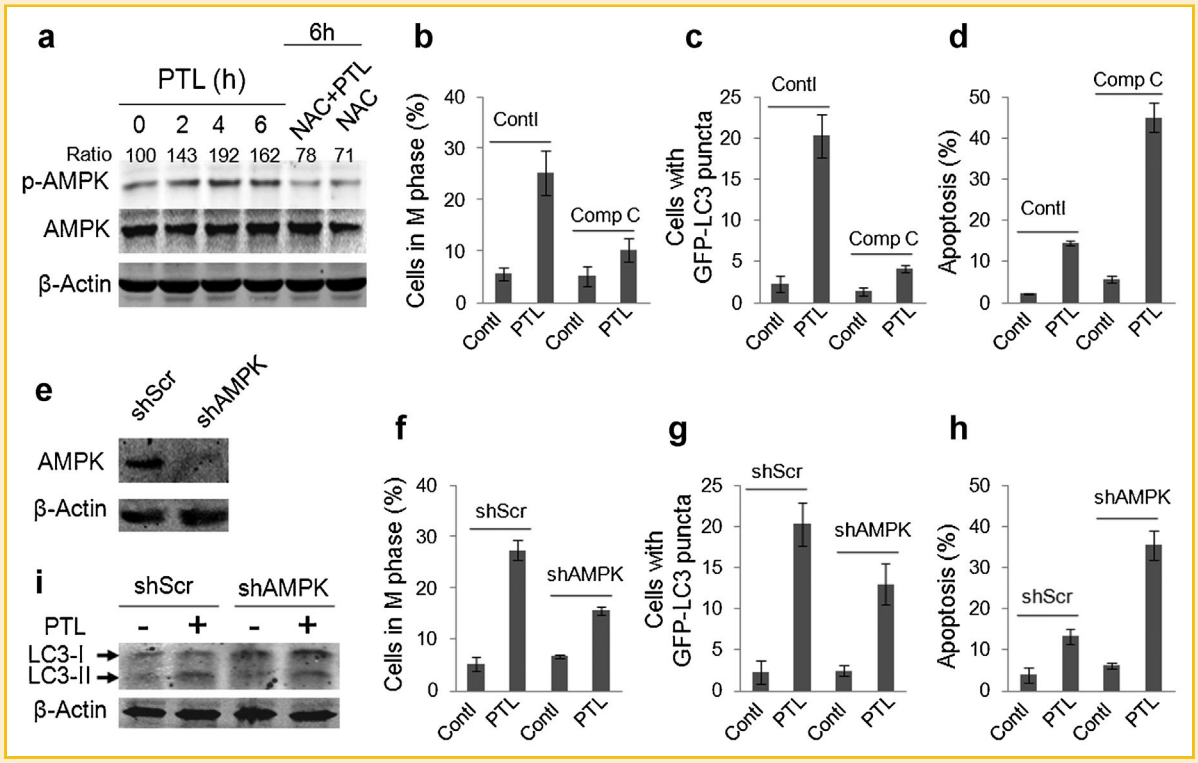

Fig. 5. PTL activated AMPK. a: MCF-7 cells were treated with 12.5 μM of PTL for the indicated periods in the presence or absence of NAC, and total and phosphorylated AMPKα protein levels were determined by Western blot analysis. The number shows the ratio of phosphorylated AMPKα to β-actin protein, because phosphorylated AMPKα represents activated kinase. b: The fraction of MCF-7/mAG-hGem(1/110) cells in M phase after treatment with 12.5 μM of PTL for 8 h in the presence or absence of 5 μM of compound C. c: The fraction of MCF-7/EGFP-LC3 cells with GFP foci after treatment with 12.5 μM of PTL for 18 h in the presence or absence of 5 μM of compound C. d: The fraction of apoptotic MCF-7/VC3AI cells after treatment with 12.5 μM of PTL for 48 h in the presence or absence of 5 μM of compound C. e: MCF-7 cells were infected with lentivirus expressing shAMPKα or scramble control (shScr). f: The fraction of MCF-7/shScr or shAMPKα cells in M phase after treatment with 12.5 μM of PTL for 8 h. g: The fraction of MCF-7/shScr or shAMPKα cells with GFP foci after treatment with 12.5 μM of PTL for 18 h. h: The fraction of apoptotic MCF-7/shScr or shAMPKα cells after treatment with 12.5 μM of PTL for 48 h. Error bar in all panels indicates ± SD (n = 3).

wide variety of cancer cells [Zhang et al., 2004; Kim et al., 2005; Liu et al., 2010]. In this report, we showed that PTL increased ROS level, activated AMPK and induced autophagy in MCF-7 cells, and that inhibition of AMPK or autophagy significantly potentiated PTL-induced apoptosis in MCF-7 breast cancer cells (Fig. 6). In fact, PTL showed the similar effects on another breast cancer cell lines, MDA-MB-231 and T47D (data not shown). Therefore, this action model of PTL might apply to breast cancers.

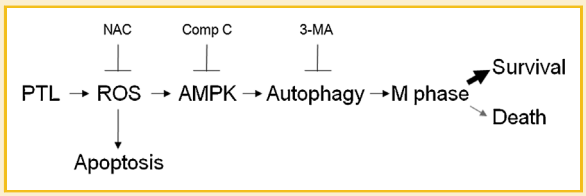

Fig. 6. A working model for PTL-induced cell death in breast cancer cells. PTL-driven ROS activates both apoptosis pathway and AMPK-autophagy survival pathway at the same time. Inhibition of AMPK or autophagy potentiates PTL-induced apoptosis in breast cancer cells. See Discussion Section for more details.

Effects of PTL on cancer cells were reported to include the inductions of ROS, cell cycle arrest, and cell death [Wen et al., 2002; Liu et al., 2010; Kreuger et al., 2012]. Here, we confirmed these effects of PTL on MCF-7 breast cancer cells. Besides, we also revealed that PTL activated AMPK pathway and autophagy. Reducing ROS suppressed all the PTL-associated events, such as cell death, AMPK activation, autophagy induction and cell cycle arrest, indicating the apical role of increased ROS in the PTL-driven cascade. Blockade of autophagy relieved cell cycle arrest, whereas inhibition of AMPK activity significantly repressed the induction of both autophagy and cell cycle arrest. Therefore, these observations clearly specify the order of PTL-induced events in MCF-7 cells, as shown in Figure 6. However, unlike ROS blockade, inhibition of either AMPK or autophagy significantly potentiated PTL-induced cell death/apoptosis in MCF-7 breast cancer cells, suggesting that PTL-activated AMPK-autophagy pathway was involved in the survival pathway. Considering that ROS scavenging inhibited cell death as well as AMPK-autophagy pathway in PTL-treated MCF-7 breast cancer cells, PTL-induced ROS appeared to activate both death pathway and survival pathway at the same time. Therefore, suppression of AMPK-autophagy survival pathway can potentially enhance PTL-induced killing of MCF-7 breast cancer cells.

ROS can be induced by a wide variety of extracellular stimuli and can potentially promote either cell survival or cell death. Here, our results showed that PTL activated both branch pathways. Although several reports have demonstrated that PTL-induced apoptosis is mediated by increased ROS level in some cancer cells, such as myeloma, leukemia, and colorectal cancer cells [Guzman et al., 2005; Wang et al., 2006; Zunino et al., 2007], the detailed mechanism largely remains to be explored. However, in other contexts, the increased ROS is often found to trigger apoptosis by targeting mitochondria [Bae et al., 2011]. Indeed, PTL-induced cell death is highly associated with some mitochondrial proteins, such as Bcl-2, Bcl-XL, and Bax, in some cell lines, such as cholangiocarcinoma and sarcoma cells [Kim et al., 2005]. Therefore, PTL-induced ROS most likely impairs mitochondrial function to elicit apoptosis, as supported by our results that Bcl-XL expression inhibited both PTL-induced ROS and cell death. On the other hand, ROS can potentially activate many kinases, such as MAPK and AMPK, and the resulting pathways possibly facilitate cell survival [Kim et al., 2013]. Our results showed that PTL activated AMPK via ROS, because antioxidant NAC totally blocked the activation of AMPK. Furthermore, our results indicated that in this context PTL-activated AMPK pathway led to autophagy and subsequential cell cycle arrest. Autophagy could be linked to cell death and survival [Rubinstein and Kimchi, 2012]. Although we found that cells arrested in M phase finally underwent cell death that at least in part resulted from non-apoptosis, blockage of AMPK or autophagy, upstream of cell cycle arrest, completely shifted cell death to apoptosis and, more importantly, significantly increased PTL-induced cell death. In fact, most of MCF-7 cells can survive from 8 h of PTL treatment, although about 25% of cells were already arrested in M phase at that time. These observations strongly suggest MCF-7 cells develop autophagy as an adaptive strategy to cope with chemical stress of PTL.

While we do not yet know the precise mechanisms underlying the induction of autophagy and cell cycle arrest by PTL-activated AMPK, previous studies on the connection between AMPK and autophagy can offer some clues [Verhulst et al., 2012]. AMPK is able to activate autophagy either by inactivating mTOR complex-1 (mTORC1) or by directly phosphorylating ULK1, a protein kinase, that initiates autophagy. Recently, a report showed that a natural compound, resveratrol, induced a G2/M phase arrest in glioblastoma that also required the induction of autophagy, which possibly involved the regulation of Cdc2, Rb, and cyclin A and B [Filippi-Chiela et al., 2011]. Thereby, it will be interesting to determine whether these pathways are involved in PTL-treated MCF-7 breast cancer cells.

Since PTL has been undergoing clinical test for its anti-cancer activity [Ghantous et al., 2010], dissection of the mechanism underneath the killing of cancer cells by PTL is very important. In the current study, we figure out a survival pathway accompanying with PTL-induced cell death in MCF-7 breast cancer cells. The competitive survival will attenuate the anti-cancer effect of the treatment. Our in vitro observations that inhibition of the survival pathway by AMPK inhibitors or autophagy blockers increases the anti-cancer activity of PTL raise the possibility that combinations of PTL and AMPK inhibitors or autophagy blockers can potentially be used as chemoprevention agents to prevent the development of breast cancers.

ACKNOWLEDGEMENTS

This work was partly supported by Grants 81171898, 81372185, and 81302080 from National Natural Science Foundation of China, 12ZCDZSY16200 from Anticancer Key Technologies R&D Program of Tianjin, 320.6700.1139 from WU JIE PING Medical Foundation.

REFERENCES

al Yacoub N, Romanowska M, Haritonova N, Foerster J. 2007. Optimized production and concentration of lentiviral vectors containing large inserts. J Gene Med 9:579–584.

Aredia F, Scovassi AI. 2013. Manipulation of autophagy in cancer cells: An innovative strategy to fight drug resistance. Future Med Chem 5:1009–1021.

Armstrong JS, Hornung B, Lecane P, Jones DP, Knox SJ. 2001. Rotenone-induced G2/M cell cycle arrest and apoptosis in a human B lymphoma cell line PW. Biochem Biophys Res Commun 289:973–978.

Bae YS, Oh H, Rhee SG, Yoo YD. 2011. Regulation of reactive oxygen species generation in cell signaling. Mol Cells 32:491–509.

Cheng G, Xie L. 2011. Parthenolide induces apoptosis and cell cycle arrest of human 5637 bladder cancer cells in vitro. Molecules 16:6758–6768.

Edinger AL, Thompson CB. 2004. Death by design: Apoptosis, necrosis and autophagy. Curr Opin Cell Biol 16:663–669.

Filippi-Chiela EC, Villodre ES, Zamin LL, Lenz G. 2011. Autophagy interplay with apoptosis and cell cycle regulation in the growth inhibiting effect of resveratrol in glioma cells. PLoS ONE 6:e20849.

Ghantous A, Gali-Muhtasib H, Vuorela H, Saliba NA, Darwiche N. 2010. What made sesquiterpene lactones reach cancer clinical trials? Drug Discov Today 15:668–678.

Gunn EJ, Williams JT, Huynh DT, Iannotti MJ, Han C, Barrios FJ, Kendall S, Glackin CA, Colby DA, Kirshner J. 2011. The natural products parthenolide and andrographolide exhibit anti-cancer stem cell activity in multiple myeloma. Leuk Lymphoma 52:1085–1097.

Guzman ML, Rossi RM, Karnischky L, Li X, Peterson DR, Howard DS, Jordan CT. 2005. The sesquiterpene lactone parthenolide induces apoptosis of human acute myelogenous leukemia stem and progenitor cells. Blood 105:4163–4169.

Huang RF, Huang SM, Lin BS, Hung CY, Lu HT. 2002. N-Acetylcysteine, vitamin C and vitamin E diminish homocysteine thiolactone-induced apoptosis in human promyeloid HL-60 cells. J Nutr 132:2151–2156.

Jain K, Paranandi KS, Sridharan S, Basu A. 2013. Autophagy in breast cancer and its implications for therapy. Am J Cancer Res 3:251–265.

Kim JH, Liu L, Lee SO, Kim YT, You KR, Kim DG. 2005. Susceptibility of cholangiocarcinoma cells to parthenolide-induced apoptosis. Cancer Res 65:6312–6320.

Kim SH, Hwang JT, Park HS, Kwon DY, Kim MS. 2013. Capsaicin stimulates glucose uptake in C2C12 muscle cells via the reactive oxygen species (ROS)/AMPK/p38 MAPK pathway. Biochem Biophys Res Commun 439:66–70.

Kim SL, Trang KT, Kim SH, Kim IH, Lee SO, Lee ST, Kim DG, Kim SW. 2012. Parthenolide suppresses tumor growth in a xenograft model of colorectal cancer cells by inducing mitochondrial dysfunction and apoptosis. Int J Oncol 41:1547–1553.

Kimura S, Noda T, Yoshimori T. 2007. Dissection of the autophagosome maturation process by a novel reporter protein, tandem fluorescent-tagged LC3. Autophagy 3:452–460.

Knight DW. 1995. Feverfew: Chemistry and biological activity. Nat Prod Rep 12:271–276.

Kreuger MR, Grootjans S, Biavatti MW, Vandenabeele P, D'Herde K. 2012. Sesquiterpene lactones as drugs with multiple targets in cancer treatment: Focus on parthenolide. Anticancer Drugs 23:883–896.

Levine B, Kroemer G. 2008. Autophagy in the pathogenesis of disease. Cell 132:27–42.

Liu JW, Cai MX, Xin Y, Wu QS, Ma J, Yang P, Xie HY, Huang DS. 2010. Parthenolide induces proliferation inhibition and apoptosis of pancreatic cancer cells in vitro. J Exp Clin Cancer Res 29:108.

Maiuri MC, Zalckvar E, Kimchi A, Kroemer G. 2007. Self-eating and self-killing: Crosstalk between autophagy and apoptosis. Nat Rev Mol Cell Biol 8:741–752.

Mathema VB, Koh YS, Thakuri BC, Sillanpaa M. 2012. Parthenolide, a sesquiterpene lactone, expresses multiple anti-cancer and anti-inflammatory activities. Inflammation 35:560–565.

Robinson JP, Carter WO, Narayanan PK. 1994. Oxidative product formation analysis by flow cytometry. Methods Cell Biol 41:437–447.

Rubinstein AD, Kimchi A. 2012. Life in the balance—A mechanistic view of the crosstalk between autophagy and apoptosis. J Cell Sci 125:5259–5268.

Russo GL, Russo M, Ungaro P. 2013. AMP-activated protein kinase: A target for old drugs against diabetes and cancer. Biochem Pharmacol 86:339–350.

Sakaue-Sawano A, Kurokawa H, Morimura T, Hanyu A, Hama H, Osawa H, Kashiwagi S, Fukami K, Miyata T, Miyoshi H, Imamura T, Ogawa M, Masai H, Miyawaki A. 2008. Visualizing spatiotemporal dynamics of multicellular cell-cycle progression. Cell 132:487–498.

Seglen PO, Gordon PB. 1982. 3-Methyladenine: Specific inhibitor of autophagic/lysosomal protein degradation in isolated rat hepatocytes. Proc Natl Acad Sci USA 79:1889–1892.

She C, Zhu LQ, Zhen YF, Wang XD, Dong QR. 2014. Activation of AMPK protects against hydrogen peroxide-induced osteoblast apoptosis through autophagy induction and NADPH maintenance: New implications for osteonecrosis treatment? Cell Signal 26:1–8.

Siegel R, Ward E, Brawley O, Jemal A. 2011. Cancer statistics, 2011: The impact of eliminating socioeconomic and racial disparities on premature cancer deaths. CA Cancer J Clin 61:212–236.

Verhulst PJ, Janssen S, Tack J, Depoortere I. 2012. Role of the AMP-activated protein kinase (AMPK) signaling pathway in the orexigenic effects of endogenous ghrelin. Regul Pept 173:27–35.

Wang W, Adachi M, Kawamura R, Sakamoto H, Hayashi T, Ishida T, Imai K, Shinomura Y. 2006. Parthenolide-induced apoptosis in multiple myeloma cells involves reactive oxygen species generation and cell sensitivity depends on catalase activity. Apoptosis 11:2225–2235.

Wen J, You KR, Lee SY, Song CH, Kim DG. 2002. Oxidative stress-mediated apoptosis. The anticancer effect of the sesquiterpene lactone parthenolide. J Biol Chem 277:38954–38964.

Wyrebska A, Szymanski J, Gach K, Piekielna J, Koszuk J, Janecki T, Janecka A. 2013. Apoptosis-mediated cytotoxic effects of parthenolide and the new synthetic analog MZ-6 on two breast cancer cell lines. Mol Biol Rep 40:1655–1663.

Yip-Schneider MT, Nakshatri H, Sweeney CJ, Marshall MS, Wiebke EA, Schmidt CM. 2005. Parthenolide and sulindac cooperate to mediate growth suppression and inhibit the nuclear factor-kappa B pathway in pancreatic carcinoma cells. Mol Cancer Ther 4:587–594.

Zhang J, Wang X, Cui W, Wang W, Zhang H, Liu L, Zhang Z, Li Z, Ying G, Zhang N, Li B. 2013. Visualization of caspase-3-like activity in cells using a genetically encoded fluorescent biosensor activated by protein cleavage. Nat Commun 4:2157.

Zhang S, Ong CN, Shen HM. 2004. Critical roles of intracellular thiols and calcium in parthenolide-induced apoptosis in human colorectal cancer cells. Cancer Lett 208:143–153.

Zunino SJ, Ducore JM, Storms DH. 2007. Parthenolide induces significant apoptosis and production of reactive oxygen species in high-risk pre-B leukemia cells. Cancer Lett 254:119–127.